Analysis of diesel fuels/biodiesel blends and identification of biodiesel using time-resolved laser-induced fluorescence spectroscopy (TRLFS)

Z. Fan, O. Schröder, and J. Krahl *

Abstract

A method based on time-resolved laser-induced fluorescence spectroscopy (TRLFS) was developed to characterize different fossil diesel fuels and biodiesel blends. The frequency behavior and decay behavior of fluorescence excited at 266 and 355 nm were measured. Differentiation of fuels was achieved by principal component analysis (PCA) of their fluorescence-lifetimes at characteristic emission wavelengths. For the quantification of biodiesel in blends, the quenching-effect on the fluorescence was determined. The results showed that the quenching-effect at the characteristic emission wavelengths (422 nm, 438 nm and 525 nm) with 355 nm laser excitation was unique for biodiesel blends. Based on that, the identification and quantification of the biodiesel was possible. TRLFS is useful for in-situ detection of the biogenic content of biodiesel blends.

Keywords: *time-resolved laser-induced fluorescence spectroscopy (TRLFS), diesel fuel, biodiesel, identification, quantification*

Zusammenfassung

Analyse und Identifizierung von Dieselkraftstoffen und Biodieselkraftstoffgemischen mittels zeitaufgelöster laserinduzierter Fluoreszenzspektroskopie (ZLIF)

Durch die zeitaufgelöste laserinduzierte Fluoreszenzspektroskopie (ZLIF) gelingt die Identifizierung verschiedener fossiler Dieselkraftstoffe und deren Mischungen mit Biodiesel. Das Frequenz- und Abklingverhalten der Fluoreszenz wurde bei Anregungswellenlängen von 266 nm und 355 nm bestimmt. Die Unterscheidung der Kraftstoffe erfolgte mittels mathematischer Hauptkomponentenanalyse (PCA). Zur Quantifizierung des Biodieselgehalts von Dieselkraftstoffen wurde der Fluoreszenzlöscheffekt genutzt.

Im Ergebnis zeigt sich, dass für Biodieselmischkraftstoffe der Fluoreszenzlöscheffekt bei Emissionswellenlängen von 422 nm, 438 nm und 525 nm unter der Anregungswellenlänge von jeweils 355 nm charakteristisch ist. Auf dieser Basis sind die Identifizierung der Biodieselsorte und die Quantifizierung der Biodieselkonzentration möglich.

Schlüsselwörter: *Zeitaufgelöste laserinduzierte Fluoreszenzspektroskopie (ZLIF), Dieselkraftstoff, Biodiesel, Identifizierung, Quantifizierung*

* Coburg University of Applied Sciences and Arts, Technology Transfer Centre Automotive Coburg (TAC), Friedrich-Streib-Straße 2, D-96450 Coburg , Germany

Contact: zhu.fan@hs-coburg.de

1 Introduction

The limited resources of fossil fuels and the negative climate impacts of greenhouse gases released from their combustion desire for alternative, renewable and CO_2-neutral fuels. One such fuel is biodiesel which produced by the triglyceride transesterification from vegetable, animal or waste oil (Knothe, 2001). Due to the variety of sources of raw materials used and natural variations of the content of the individual ingredients in raw materials, the optimum performance and emissions of diesel engine operation is a particular challenge. Therefore, it is of great economic and ecological importance to identify biodiesel in diesel fuel blends to achieve optimum performance and emissions.

In this context Munack and Krahl developed a biodiesel sensor which enables to determine the concentration of biodiesel (main components are Fatty Acid Methyl Ester – FAME) in conventional diesel fuel. The sensor operates on the measurement of the dielectric number and is suitable for biodiesel and its blends with diesel fuel as well as for the quantification of ethanol in gasoline (Munack and Krahl, 2003). However this sensor could not identify the composition of conventional diesel fuel and biodiesel.

Some analytical laboratory techniques, e. g. GC-MS and HPLC, can analyze the fuel components (Glover and Bullin, 1989; Plank and Lorbeer, 1995; Lechner et al., 1997; Foglia et al., 2005). However these techniques need sample preparation and are cost and time intensive, so that they cannot be applied for in-situ detection of fuels.

Chuck et al., 2010 report about FT-IR spectroscopy, refractive index and UV-vis spectroscopy to determine biodiesel in blends. Their work showed that FT-IR could be used on-vehicle for the determination of biodiesel content with refractive index measurement providing the fatty acid composition. However because of the cost and complexity both techniques may not be commercially viable. Application of UV–vis for on-vehicle is not considered feasible (Chuck et al., 2010).

The aim of this paper is to introduce fluorescence sensing technology to identify different fuels and their biodiesel blends. Methods based on fluorescence spectroscopy are easy to use and provide quick and accurate results (Hengstermann and Reuter, 1980; Barbini et al., 1992; Camagni et al., 1991; Patsayeva et al. 2000; Steffens et al., 2011; Scherer et al., 2011; Ralston et al., 1996; Kulkarni et al., 2008; Zawadzki et al., 2007) and may be also used in the future to identify the fuels and determine biodiesel content in the blend. However, these methods are challenging in remote sensing application because it requires the use of tunable lasers which usually have too weak inten-sities (Quinn et al., 1994; Ryder et al., 2002).

A method of time-resolved laser-induced fluorescence spectroscopy is suitable for remote sensing applications using an intense pulsed Q-switched laser. It has been applied in the identification of fossil fuels (Hegazi et al., 2005; Jacob et al., 2006). Spectral characterization of crude oils was attempted by using the contour diagrams of equal fluorescence intensities. This served as unique fingerprints for the crude oils from the TRLFS-techniques (Hegazi and Hamdan, 2002; Hegazi et al., 2005).

Due to interference of the individual spectra by numerous fluorophores, fluorescence of diesel fuels is complex. The compounds with large conjugated double-bonds or benzene rings are major sources of fluorescence in diesel fuel. The absorption of light in the conjugated system excites a π-electron into an anti-bonding π^* orbital (π-π^* transition). The fluorescence peaks of aromatic compounds are therefore shifted to longer wavelengths (red shift) with increasing alkylation (Dumke and Tescher, 1988; Khorasani, 1987).

The fluorescence lifetime from the TRLFS-measurements characterizes the unique fluorescence property of the fluorophores in diesel fuels and biodiesel blends. Therefore, it can be used for characterization and identification of fuels (Fan and Krahl, 2013). In our previous work we found that TRLFS with 266 nm pulsed laser excitation was able to detect and distinguish the fossil diesel fuels and the biogenic fuels; especially the blends with different biogenic content.

Just like the technique of face recognition and fingerprint identification, for the exploratory analysis of the oils and fuels by the means of fluorescence spectroscopy, the principal component analysis (PCA) can be applied (Guimet, 2005; Schmid, 2009; Sikorska et al., 2012; Fan et al., 2013). PCA was invented in 1901 by Karl Pearson (Pearson, 1901) and the application has been widely described in literature (Bünting, 1999; Jolliffe, 2002; Scott et al., 2003; Guimet, 2005; Schmid, 2009; Kongbonga et al., 2011; Sikorska et al., 2012).

Hence the PCA-technique was used to analyze a two-way matrix of life times. With this method, we achieved a quick and accurate analysis. The result makes the TRLFS-method attractive for online identification of diesel fuels and biodiesel blends.

Caires et al. (2012) reported on quantification of biodiesel content in biodiesel blends by a fluorescence spectrophotometer. In their work, the different blends were prepared from four refined vegetable oils (canola, sunflower, corn and soybean biodiesel; biodiesel content up to 10 % v/v). Using a fluorescence spectrophotometer with excitation at 260 nm, the fluorescence behavior at about 470 nm was same for all blends. This means that quantification of biodiesel based on the fluorescence method at this emission wavelength is independent of the vegetable oil feedstock. However, it is still doubtful whether this conclusion is really true for other FAME. In our previous work, the fluorescence intensity of blend from CEC Reference Diesel Fuel (DF_{Ref}) and RME at the emission wavelength of maximum intensity (338 nm) excited by the 266 nm laser was measured. Very little RME fluorescence was found by the TRLFS at 266 nm laser excitation. We reported that the fluorescence quenching-effect must be considered in determining biodiesel concentrations (from 0 % to 100 % v/v) in biodiesel blends (Fan and Krahl, 2013). This means that at least the fluorescence behavior of RME was not same as the other FAME.

Rapeseed oil and soybean oil are the most important vegetable raw materials for biodiesel in Germany (Bockey, 2013). So blends with biodiesel from rapeseed oil methyl ester were preferentially studied in this work and soybean oil methyl ester (SME) as well, because of its importance for

South Europe and North America. Clear fluorescence could be detected for both biodiesels (RME and SME) when using the TRLFS-technique with 355 nm laser to detect differences between fluorescence intensity and content of two biodiesels. Moreover, when excited by the 355 nm laser, the quenching-effect of biodiesel turned out to be unique. Based on this, not only the identification but also the quantification of biodiesel in the biodiesel blends could be determined.

2 Spectroscopic methods and materials

2.1 Theoretical background

The fluorescence emission in time-resolved measurements can be described like monomolecular reactions if the laser pulse width is very short. Thus, the temporal emission can be described by the simple exponential decay function $I(t)$ with fluorescence lifetime τ (Lampert et al., 1983; Lakowicz et al., 1991):

$$I(t) = I_{t=0} \cdot e^{\left(-\frac{t}{\tau}\right)} \quad (1)$$

Where $I_{t=0}$ is the fluorescence intensity at $t = 0$.

According to this equation, the fluorescence lifetime is the time at which the fluorescence intensity is decayed to 1/*e* (~ 36.8 %) of the original value.

In practice, the influence of the laser pulse width on the fluorescence lifetime must be considered. In this case, the experimentally measured $I_{exp}(t)$ is not the true fluorescence response function from the sample under investigation. The experimentally recorded $I_{exp}(t)$ is a convolution of the instrument response function (excitation laser pulse) $I_{pulse}(t)$ and the exponential decay function $I(t)$ (Grinvald et al., 1974; Terzic et al., 2008):

$$I_{\exp}(t) = \int_0^t I_{pulse}(t') \cdot I(t - t')dt' \quad (2)$$

For a complex mixture of *N* fluorophores, $I(t)$ is the sum of fluorescence intensities of all fluorophores *i*:

$$I(t) = \sum_{i=1}^{N} I_{i,t=0} \cdot e^{\left(-\frac{t}{\tau_i}\right)} \quad (3)$$

This equation is in accordance with Linear-Mixture-Model (LMM) (Bünting, 1999; Martens and Naes, 1998) which is the basis for the analysis of the overlaying or interfering signals in this work.

With PCA, an orthogonal linear transformation of observations of the correlated variables into values of uncorrelated variables in a new coordinate system can be made. In this system, the greatest variance of the data is on the first coordinate (also called the first principal component, PC1), the second greatest variance on the second perpendicular coordinate, and so on. The number of principal components should be much less than the number of original variables. From PCA analysis, usually the terms of component scores also called factor scores (the transformed variable values corresponding to a particular data point), and loadings (the weight by which each standardized original variable should be multiplied to get the component score) are obtained (Pearson, 1901; Jolliffe, 2002; Abdi et al., 2010). The unfold principal component analysis (U-PCA), also named multi-way principal component analysis, is usually applied to analyze a two-way matrix ($\in IR^{I \times (J \times K)}$) obtained after unfolding a three-way array ($\in IR^{I \times J \times K}$) (Westerhuis et al., 1999; Henrion, 1994). In this example, a data set of TRLFS-measurements is "I" the number of samples, "J" the number of emission lengths (λ_{EM}) and "K" the number of decay times. In this work, the life times of different fuels were calculated from the TRLFS-spectra and a two-way array ($\in IR^{I \times F}$) was built. Here "F" is the number of selected emission wavelengths at which the lifetime was calculated. Then the dataset was analyzed using the PCA-technique. Compared to the U-PCA, this process avoided unfolding the spectra and also greatly reduced amount of data.

In this work the TRLFS-data were processed using the software MATLAB (MathWorks R2010b).

2.2 Measuring system

The TRLFS system, OPTIMOS, delivered by Optimare (Wilhelmshaven, Germany) is based on the pulse method (time domain) and harmonic wavelength generation.

The remote sensing experimental setup is shown in Figure 1. All components of the OPTIMOS (Nd:YAG laser with Q-switch, harmonic generator, delay generator, detector (ICCD camera with spectrograph) and computer) are integrated into an aluminum rack with operation panel. The OPTIMOS-system has been described in the literature (Optimare , 2005; Fan and Krahl, 2013).

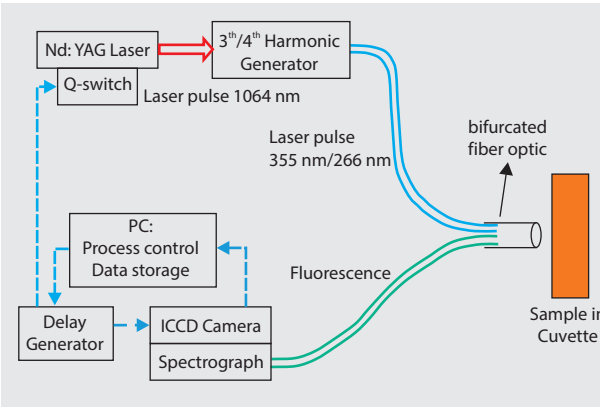

Figure 1
Schematic diagram of remote sensing experimental setup of OPTIMOS-System

The TRLFS measurement was performed on diesel fuels in a quartz cell. The emission spectra of different diesel fuels were

recorded in the range 200 to 600 nm with a specific time gate width (2 ns) and gate step (2 ns) excited at 266 and 355 nm.

2.3 Fuels

Most of the fuels were bought from filling stations or delivered by mineral oil or biofuel companies (e.g. Shell, Aral, China National Petroleum Corporation CNPC) in Europe, Asia and North/South America. Additionally, the Thünen Institute of Agricultural Technology, Braunschweig, Germany, delivered different biodiesel qualities and blends of conventional and advanced biofuels. The fuels were analysed by TRLFS without any prior treatment. To validate how specific the fluorescence of diesel fuel brand is, the fluorescences of the diesel fuel brand from up to five filling stations were tested. No significant differences were detected between the different filling stations. For study of the dependence between fluorescence intensity and biodiesel content, we prepared different biodiesel fuel blends (0 to 100 % v/v).

3 Results

3.1 Exploratory analysis of diesel fuels

3.1.1 TRLFS-spectra of diesel fuels

Figure 2 shows 3D-TRLFS fluorescence spectra of nine different fuels with pulsed 266 nm laser excitation (top, left to right: Aral Diesel (up to 7 % biodiesel), Aral Ultimate Diesel (biodiesel free, new generation high performance diesel fuel), Shell V-Power Diesel (biodiesel free, new generation high performance diesel fuel); middle: Co-ordinating European Council (CEC) Reference Diesel Fuel by Haltermann (DF_{Ref} , ca. 20 % aromatics), Biodiesel Blend (blend of CEC Reference Diesel, Biodiesel RME and Octanol), hydrotreated vegetable oil HVO (Neste Oil); bottom: Diesel Fuel from CNPC in South China, Diesel Fuel from Argentina, Swedish miljöklass 1 (MK1, aromatics free). These spectra represent fluorescence intensities with color bar as a function of wavelength (x-axis) and decay time (y-axis).

In contrast to the set of 3D-TRLFS spectra with 266 nm excitation, the fluorescence spectra for the same nine fuels with pulsed 355 nm laser excitation are shown in Figure 3.

In Figures 2 and 3, the discriminations of the shapes in the TRLFS spectra are clearly visible to differentiate with both excitations between diesel fuels and their blends with biodiesel. However, it should be noted that for the TRLFS measurement with 355 nm laser excitation, the signals of some fluorophores were lost or shaded out. These fluorophores are usually PAH with two or three aromatic rings (for example, Acenaphthene, Fluorene, Phenanthrene and Naphthalene) or the derivatives of PAH (for example, 1,3-Dimethylnaphthalene and 1,6-Dimethylnaphthalene). Their emission wavelengths are usually shorter than 355 nm (Bünting, 1999; Jacob et al., 2006; Fan et al., 2013). Therefore, it is recommended that for analysis of fluorescence spectra of diesel fuels, the 266 nm laser should be used.

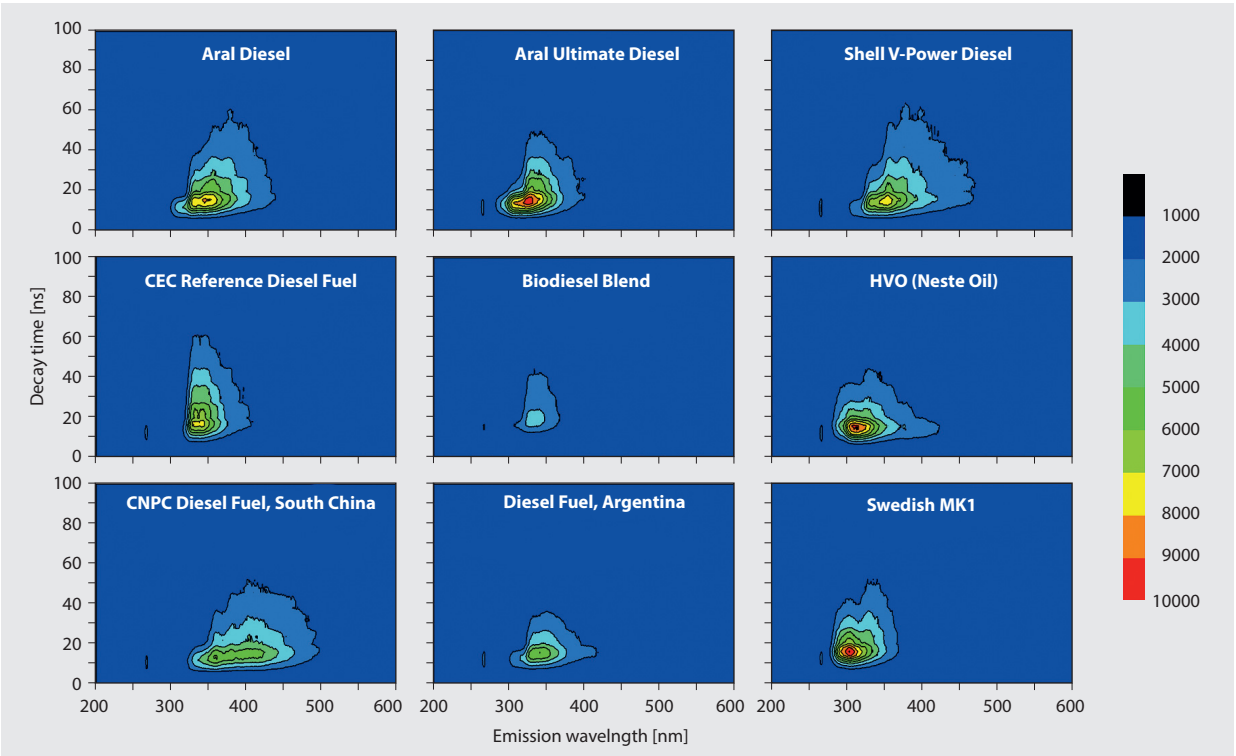

Figure 2
3D-TRLFS fluorescence spectra of nine different fuels, excitation at 266 nm

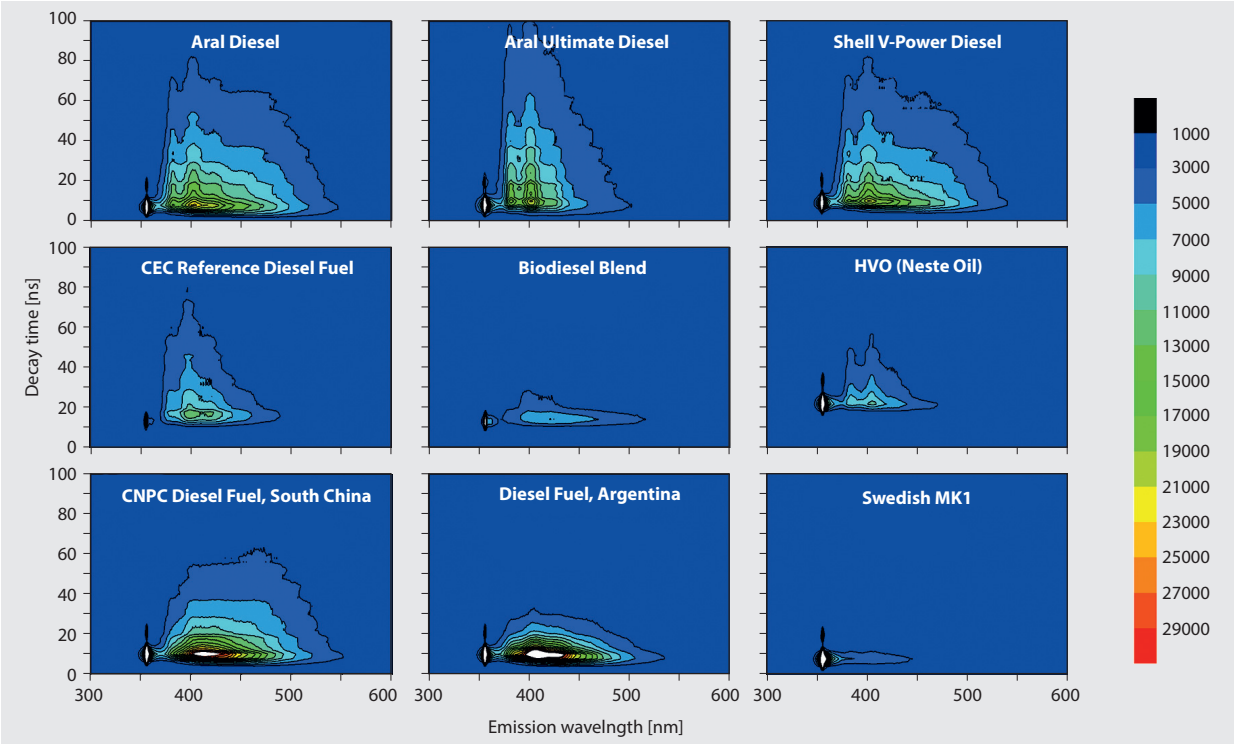

Figure 3
3D-TRLFS fluorescence spectra of nine different fuels, excitation at 355 nm

3.1.2 Principal component analysis

The fluorescence lifetimes for characteristic emission wavelengths were calculated. The characteristic emission wavelengths are the minimal wavelengths at which a maximum fluorescence of a fuel was detected. By comparing the spectra of these diesel fuels and biodiesel blends, nine characteristic emission wavelengths (300, 328, 340, 355, 377, 396, 407, 414 and 423 nm) were selected. The fluorescence lifetimes for these characteristic emission wavelengths were calculated from the decay curve $I_\lambda(t)$. The mean fluorescence lifetimes of the different fuels are listed in Table 1.

As mentioned above, the loadings from PCA-method of the measured original variables (fluorescence lifetimes) of fuels could build a new coordinate system and their scores represent the transformed values of original variables in the new coordinate system. A differentiation of these diesel fuels and biodiesel fuel blends can be obtained by analysis of fluorescence lifetime database using the PCA method.

The score biplot of the first two principal components PC1, PC2 (86.1 % of explained variance) is shown in Figure 4. It shows that the score of the first two principal components of diesel fuels can be well distinguished. That is, first, the score-cluster of same fuels is within a certain range. Second, the score-cluster of diesel fuels can be separated from each other very well.

Table 1
Mean lifetimes (in nanoseconds) of nine fuels at characteristic emission wavelengths

Fuels	Emission wavelengths [nm]								
	300	328	340	355	377	396	407	414	423
Aral Diesel	15	12	12	19	29	37	36	39	41
Aral Ultimate Diesel	7	16	16	18	35	57	58	69	82
Shell V-Power Diesel	14	14	15	22	34	44	44	45	49
CEC Reference Diesel Fuel (DF_{Ref})	27	23	22	24	37	54	47	48	48
Biodiesel Blend from DF_{Ref}, RME and Octanol	14	24	24	28	40	64	53	76	102
HVO (Neste Oil)	12	16	19	21	22	22	21	22	23
CNPC Diesel Fuel, South China	45	9	9	15	21	22	22	22	24
Diesel Fuel, Argentina	14	11	11	13	16	17	16	18	18
Swedish MK1	11	21	26	31	33	40	39	48	55

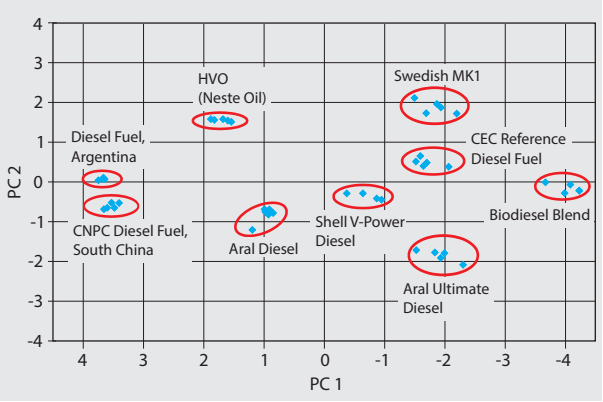

Figure 4
Score biplot from PCA of the first two principal components (PC1: 70.6 % und PC2: 15.5 %)

These nine diesel fuels and biodiesel blends are separated mainly along PC1. Diesel Fuel, Argentina and CNPC Diesel Fuel, South China have the most negative scores; in contrast Biodiesel Blend has the most positive scores.

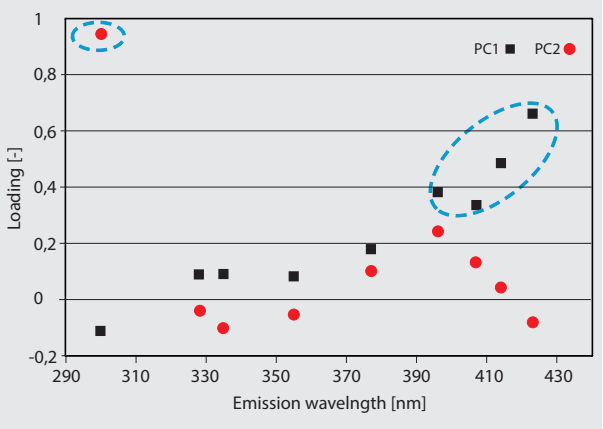

Figure 5
Loading plot from PCA of PC1 and PC2 of the fluorescence lifetime matrix at nine emission wavelengths

The loadings in Figure 5 indicate that a high score in PC1 (70.6 % variance is explained) is mostly related to high emission wavelengths (396, 407, 414 and 423 nm). The fluorescence in the wavelength range was related to PAH with more than three benzene rings (for example, chrysene, dibenz [a,h] anthracene, Benzo [g,h,i] perylene or their derivatives) (Ma et al., 1996; Fan et al., 2013). Despite their low content in the reference diesel fuel (< 0.1 % (m/m), see Appendix A), the fluorescence life time could be determined very well and used to identify diesel fuels, because fluorescence is a very sensitive technique and TRLFS provides excellent measurement stability for the fluorescence life time. The most positive scores of Biodiesel Blend have the longest fluorescence lifetime at these high emission wavelengths. Also the most negative scores in PC1 of Diesel Fuel, Argentina and CNPC Diesel Fuel, South China have the shortest fluorescence lifetimes at these emission wavelengths.

Conversely, a high score in PC2 (15.5 % variance is explained) is mostly related to a low emission wavelength (300 nm). The fluorescence at this wavelength was related to PAH with two or three benzene rings (e g. naphthalene, fluorine, anthracene or their derivatives). PC2 doesn't distinguish the diesel fuels as well as PC1, however, it can be seen that HVO (Neste Oil) and Swedish MK1 (which have the most positive scores in PC2) own the longest fluorescence lifetime at low emission wavelength (300 nm). The most negative score in PC2 of Aral Ultimate Diesel had the shortest fluorescence lifetime of 300 nm.

For comparison, U-PCA of the emission spectra of fuels between λ_{EM} = 300 nm and 530 nm, as well as decay time from 0 to 200 ns, was carried out. The wave length step is 0.383 nm and decay time step is 2 ns. The dimension of a TRLFS spectrum is 624 x 101. The variances accounted for the first two PCs for both analyses and are shown in Table 2.

Table 2
Percentage of explained variance of the PCA and U-PCA models

PCA[a] (life times at nine EMs)		U-PCA[b] (time-resolved emission spectra)	
PC1	PC2	PC1	PC2
70.6 %	15.5 %	47.8 %	31.1 %

a: matrix dimension of life times: 9 x 9
b: matrix dimension of a TRLFS spectrum: 9 x 63024

This shows that for PCA of the life time of fuels, PC1 and PC2 cumulatively explained 86.1 % of the total variance. For U-PCA of the emission spectra of fuels this value was by contrast 78.9 %.

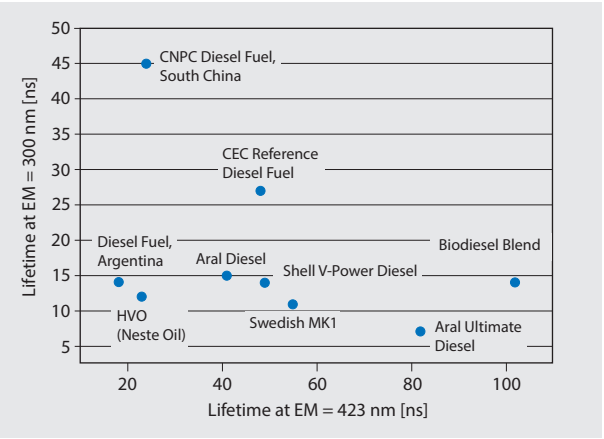

Figure 6
Biplot of the mean fluorescence lifetimes (at EM = 300 nm und 423 nm) of nine fuels

It is possible to distinguish the different diesel fuels and biodiesel fuel blends by their lifetimes at characteristic

wavelengths (300 nm and 423 nm), because the PC1 and PC2 is mostly based on the fluorescence lifetime of these wavelengths. Figure 6 shows a biplot of mean fluorescence lifetimes at these wavelengths from Table 1.

It shows that, just like PCA, by using the two fluorescence lifetimes, that these diesel fuels can be easily well distinguished. Biodiesel Blend has the longest fluorescence lifetime at EM = 423 nm. In contrast, Diesel Fuel, Argentina, CNPC Diesel Fuel, South China and HVO (Neste Oil) have short lifetimes. This correlates to the analysis by PC1 (Figure 4).

At EM = 300 nm, Aral Ultimate Diesel showed the shortest fluorescence lifetime. It is also in parallel to the analysis by PCA. In contrast to PCA, CNPC Diesel Fuel, South China and CEC Reference Diesel Fuel have the longer lifetimes.

3.2 Identification of biodiesel in biodiesel blends

According to Beer's law and the Linear-Mixture-Model under constant experimental conditions (e. g. temperature, pressure, pH), when a fluorophor is analyzed at low concentrations in a homogeneous solution with negligible matrix interference, a simple relationship between fluorescence intensity I_f at a given emission wavelength and biodiesel concentration BX (X is the percentage of biodiesel blended) is given by the following formula (4):

$$I_f = I_{fossil} \cdot (1 - BX) + I_{bio} \cdot BX = k \cdot BX + b \quad (4)$$

Here I_{fossil} and I_{bio} are the fluorescence intensity of pure fossil diesel and pure biodiesel.

To determine the biodiesel content in diesel fuel, blends (B0, B5, B7, B10, B20, B30, B40, B50, B60, B70, B80, B90, B92, B95, B98, B100) were prepared from CEC Reference Diesel Fuel (DF_{Ref} , Appendix A) and biodiesels (RME and SME, Appendix B).

Figure 7 shows that with 266 nm excitation, the fluorescence for the ultraviolet and visible region derived only from the CEC Reference Diesel Fuel and not from RME or SME since the fluorescence of the possible fluorophore (Vitamin E, natural antioxidants) in biodiesel at excitation of 266 nm was undetectable. The TRLFS-spectrum of neat reference diesel showed that the emission wavelength for the maximum fluorescence intensity was 340 nm. Therefore, for the excitation wavelength of 266 nm, the diesel fuel content in fuel blend could be referred to by the fluorescence intensity at the emission wavelength of 340 nm. The biodiesel content can be indirectly calculated using Formula (4).

At 355 nm excitation, the fluorescence derives both from the reference diesel fuel, RME and SME (Figure 8). The emission wavelength for the maximum fluorescence inten-sity of neat reference diesel is 422 nm. At this emission wavelength, there is no fluorescence from RME. The emission wavelength for the maximum fluorescence intensity of neat RME is 525 nm, which belongs to Vitamin E (Kyriakidis and Skarkalis, 2000; Sayago et al., 2004; Kongbonga, et al. 2011). For neat SME, there are strong fluorescences between 400 nm and 500 nm, which correspond to the remaining fluorophores (oxidation products or tocopherols) of SME from refinement processes (Sayago et al., 2004; Kongbonga et al., 2011). The emission wavelength for the maximum fluorescence intensity of neat SME is 438 nm.

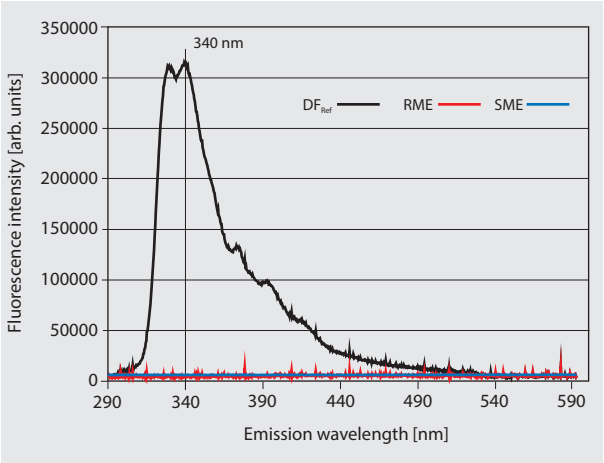

Figure 7
Fluorescence frequency behavior of CEC Reference Diesel Fuel (DF_{Ref}) and biodiesel fuel RME under excitation at 266 nm

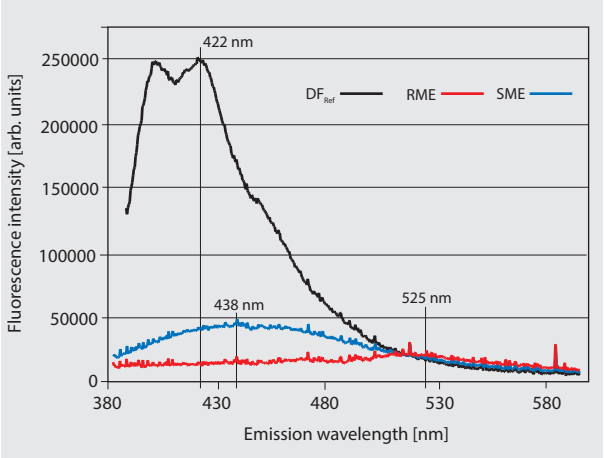

Figure 8
Fluorescence frequency behavior of CEC Reference Diesel Fuel (DF_{Ref}), RME and SME under excitation at 355 nm

For the excitation wavelength of 355 nm, the fossil diesel fuel content in fuel blend could be determined by the fluorescence intensity at the emission wavelength of 422 nm. In contrast, the content of RME in fuel blend could be determined by the fluorescence intensity at the emission wavelength of 525 nm. The content of SME could be referred at the emission wavelength of 438 nm. It is noticeable that the fluorescence intensity at 438 nm from fossil diesel fuel is about three times higher than that from SME. The emission bands observed in diesel are principally due to aromatic

compounds/conjugated double bonds and could be a strong influence on the fluorescence of SME. The fluorescence intensity from fossil diesel fuel at 525 nm is similar to that from RME. So it is possible that there is an influence on the fluorescence of RME by fossil diesel.

3.2.1 Measurement with 266 nm laser excitation

The fluorescence intensities (with 266 nm laser excitation) are normalized to the maximum value of the pure fossil diesel (at 340 nm). The fluorescence at 340 nm can be ascribed to PAH in CEC Reference Diesel Fuel. The normalized fluorescence intensity for the emission wavelength of 340 nm is plotted against the concentration of RME (Figure 9).

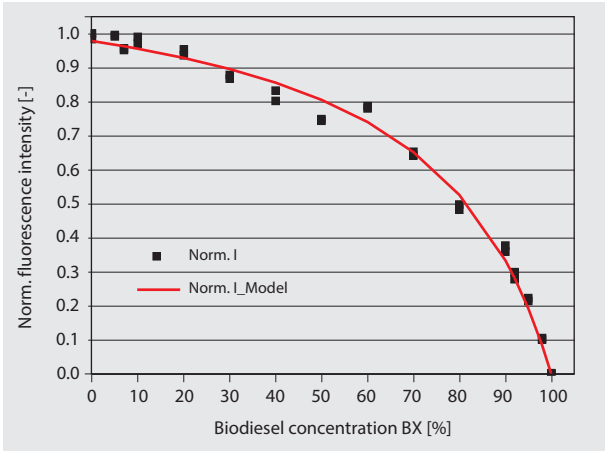

Figure 9
Adaption of the Stern-Volmer equation with normalized fluorescence intensity for the given emission wavelength of 340 nm versus content of RME in Biodiesel Blend, excitation at 266 nm

It was observed that the fluorescence intensity decreased in general with the increase of biodiesel concentration. However, there were some differences: the fluorescence of the blends was higher than expected (above the diagonal, see Figure 9). The possible reason being secondary absorptions by the compounds in fuels. Figure 9 showed a change of the gradient in dependency of the biodiesel concentration. Especially at low biodiesel concentrations (B0 to B30), when the amount of concentration of fluorophores in the blends is very high, the fluorescence will be quenched by the fluorophores. This means that the fluorescence of blends with low biodiesel concentration increases were not as strong as with high biodiesel concentration. This phenomenon is similar to the static self-quenching of fluorophores.

Generally, the static quenching effect can be described by the Stern-Volmer equation (Somoogyi et al., 1993; Lakowicz, 2010; Eftink, 1991; Eftink et al., 1981; Lakos et al., 1995):

$$\frac{I_{f,0}}{I_f} = \frac{k_1 \cdot [FL] + k_2 \cdot BX}{I_f} = 1 + K_{SV} \cdot [Q] \qquad (5)$$

Here $I_{f\,0}$ is the fluorescence intensity without quenching and has a linear dependence with fossil diesel concentration $[FL]$ and biodiesel concentration BX with factor k_1 and k_2. I_f is the fluorescence intensity with quenching. K_{SV} is the Stern-Volmer constant and $[Q]$ is the quencher concentration. For self-quenching the fluorophore concentration $[FL]$ is equal to $[Q]$.

By fitting the Stern-Volmer equation with the experimental data, the two constants were determined: K_{SV} = 3.66, k_1 = 4.56 and k_2 = 0. From Figure 9, it can be found that the Stern-Volmer equation was very well adapted to the experimental data.

3.2.2 Measurement with 355 nm laser excitation

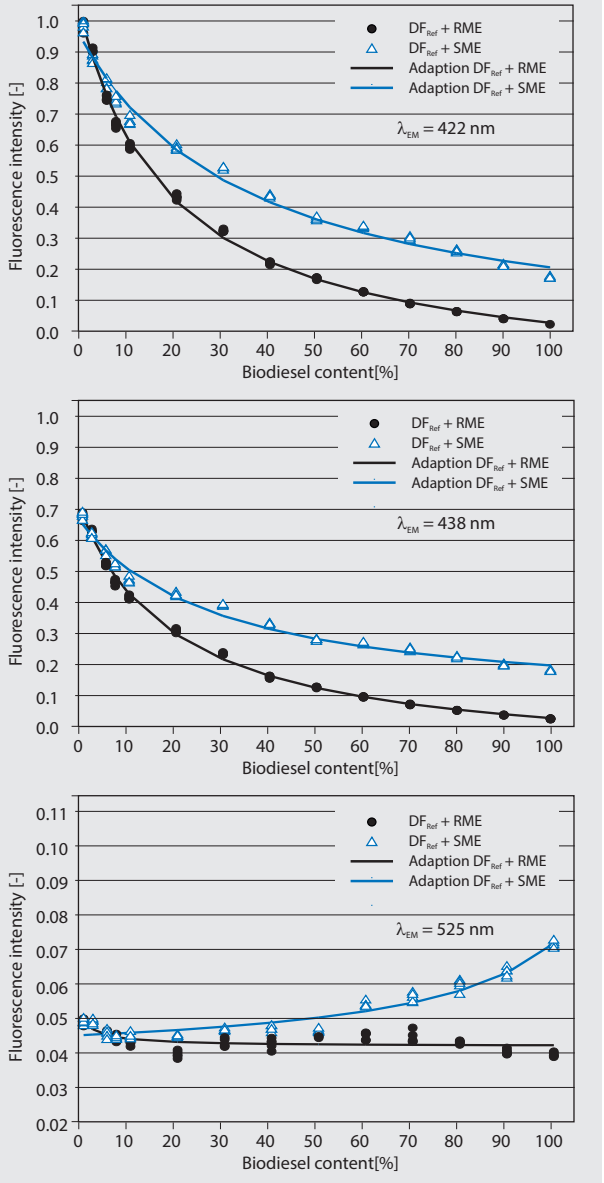

Figure 10
Adaption of the Stern-Volmer equation with experimental data of blends, for the given emission wavelength of 422 nm (top), 438 nm (centre) and 525 nm (bottom)

The fluorescence intensities (at 355 nm laser excitation) were normalized to the maximum value of the pure fossil diesel (at 422 nm). Then, the normalized values for the emission wavelengths of 422 nm, 438 nm and 525 nm were plotted against the biodiesel concentration (Figure 10).

The fluorescence with the emission maximum at 422 nm was ascribed to the CEC Reference Diesel Fuel. The fluorescence at 438 nm can be ascribed both to the fluorophores of SME and the CEC Reference Diesel Fuel. The fluorescence at 525 nm was ascribed to the fluorophores of RME.

It was observed, that for the blends, the fluorescence intensities at 422 nm did not show a linear relation with the content of biodiesel because of the strong secondary absorption of biodiesel. This quenching effect of biodiesel could be solved by the Stern-Volmer model. At the other emission wavelengths of 438 nm and 525 nm, the relation between the fluorescence intensity and biodiesel content could also be described by the Stern-Volmer equation (Figure 10). The results of model analysis were verified by the results of experiments. The parameters of the Stern-Volmer equation are shown in Table 3. The quenching-effect is unique for the blends with different diesel and biodiesel at varying concentrations. At 525 nm wavelength, the blends whose data were fitted using the Stern-Volmer equation showed a general trend. This was because the fluorescence intensity of all fuels was in the same range and near the noise level. Therefore, only a general trend was noted after using the Stern-Volmer equation.

Table 3
Parameters fitted for the Stern-Volmer equation for emission wavelengths at 422, 438 and 525 nm

Blends	EM	k_1	k_2	K_{SV}
DF_{Ref} + SME	422 nm	0.9337	0.7599	2.7100
	438 nm	0.6511	0.8445	3.3365
	525 nm	0.0454	0.0169	-0.7658
DF_{Ref} + RME	422 nm	0.9854	0.1487	4.8279
	438 nm	0.6796	0.1397	4.7092
	525 nm	0.0496	1.1088	25.1363

In Figure 11, the diagram of fluorescence intensities for biodiesel blends are shown for these emission wavelengths. Although only a general trend for the dependence between fluorescence intensity at EM = 525 nm and biodiesel concentration could be found, the distinction of the blends at this wavelength was so significant that the fluorescence at this wavelength could be used to identify the blends. The results suggest that the fluorescence at three characteristic emission wavelengths (422 nm, 438 nm and 525 nm) could be used for identification and quantification of biodiesel.

In order to validate this assumption, these fluorescence intensities and the correspondent concentrations were used as training dataset for a calibration to quantify the biodiesel content in unknown blends.

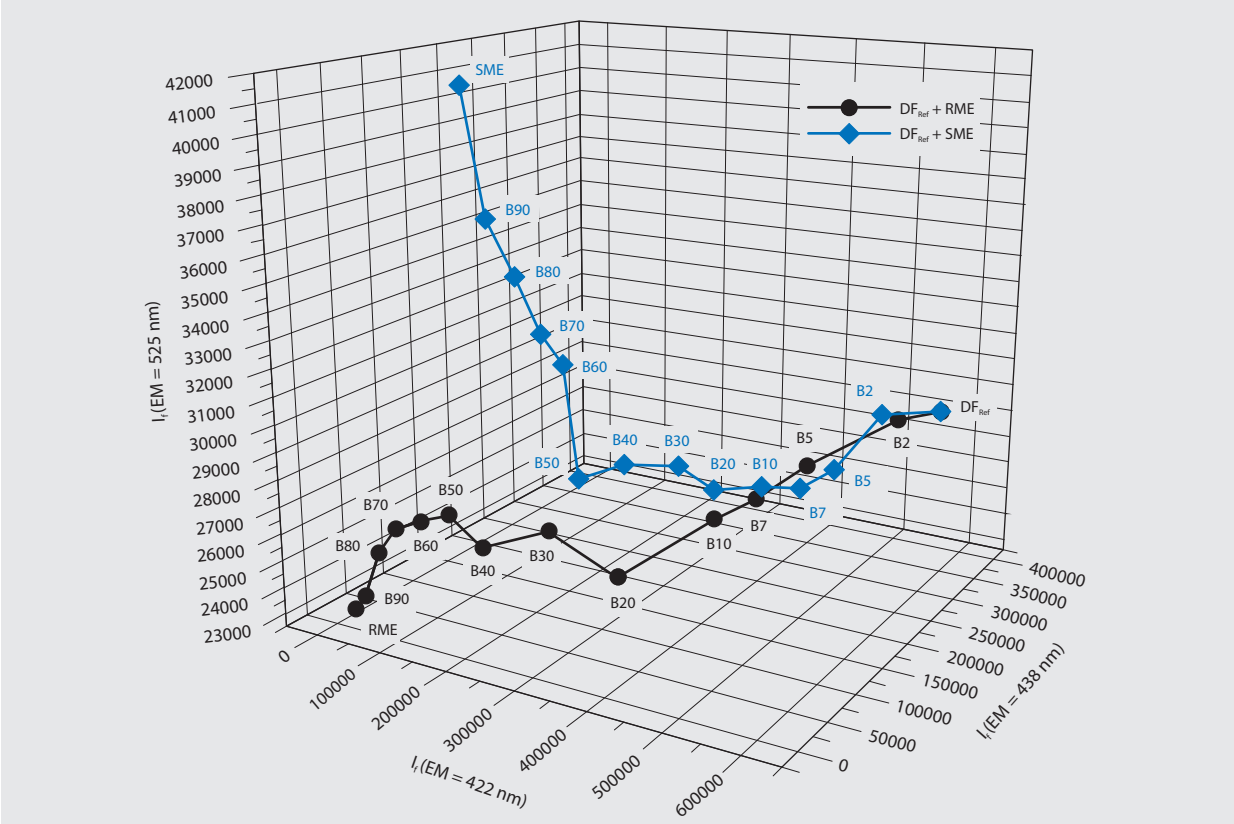

Figure 11
3D diagram of fluorescence intensities for the biodiesel blends

3.2.3 Validation

This calibration was tested with blended samples with different biodiesel content. In all, 40 test samples were mixed consisting of DF_{Ref} and SME or DF_{Ref} and RME to evaluate the true predictive ability of the calibrated model. Identification and quantification of biodiesel in the test samples were carried out according to the similarity of the test samples by the variables (I_f(EM = 422 nm), I_f(EM = 438 nm) and I_f(EM = 525 nm)) with the calibration samples. In this work, we used Euclidean distance, D, between test samples i and known samples j to indicate the similarity (Vandeginste et al., 1998):

$$D_{i,j} = \sqrt{\sum_{k=1}^{K} \left(I_{f\,i,k} - I_{f\,j,k} \right)^2} \qquad (6)$$

where K is the number of variables, here it is 3.

The smallest distance D_{min1} means the test sample was almost similar to the corresponding known sample. Thus according to the D_{min1} the biodiesel in the blend could be identified. Also the second smallest distance D_{min2} could be calculated. Finally, according to D_{min1} and D_{min2}, the biodiesel content c in test blend could be calculated: using a linear interpolation between these two known concentrations (BX_1 and BX_2):

$$\frac{D_{\min 1}}{D_{\min 2}} = \frac{c - BX_1}{c - BX_2} \Rightarrow c = \frac{\left(BX_2 \cdot D_{\min 1} - BX_1 \cdot D_{\min 2} \right)}{\left(D_{\min 1} - D_{\min 2} \right)} \qquad (7)$$

The results of quantification of DF_{Ref}, RME and SME in biodiesel blends are shown in Figure 12, 13 and 14. Table 4 shows the prediction ability for identification of biodiesel type.

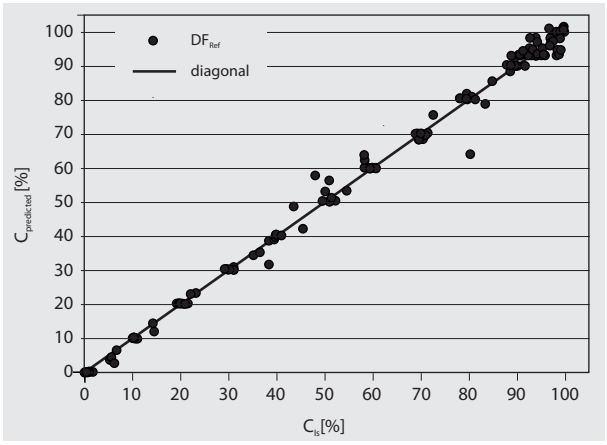

Figure 12
Predicted vs. true concentration for DF_{Ref} in biodiesel blends

Fossil diesel can (Figure 12 and Table 4) be identified and quantified even at low concentrations (DF_{Ref} % smaller than 1 %). RME and SME (Figure 13, Figure 14 and Table 4) in most blends could also be determined. Table 4 shows the high identification ability of this method: more than 90 % of the fuels were identified.

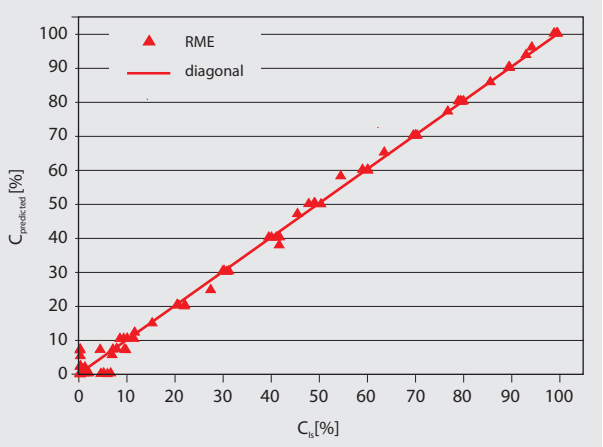

Figure 13
Predicted vs. true concentration for RME in biodiesel blends

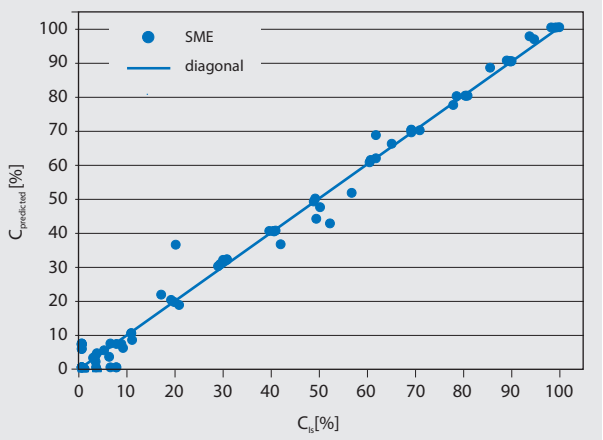

Figure 14
Predicted vs. true concentration for SME in biodiesel blends

Table 4
Prediction ability for identification of biodiesel type in biodiesel blends.

	DF	RME	SME
true	40	37	37
false	0	3	3

It should be noted that the high residuals (greater than 10) were caused by false identification of biodiesel. For example, a blend of 93 % DF_{Ref} and 7 % RME, showed that there should be 85 % DF_{Ref} and 15 % SME. Therefore, a high residual occurred. It means that correct identification of biodiesels plays a very important role for the quantification. Therefore, the

identification method needs to be improved. For example, the expansion of the measuring range of emission wavelength in the detector and adjustment of the wavelength of the laser light may need improvements.

4 Conclusions

In this work, the fluorescence properties of over 50 diesel fuels and biodiesel mixtures were determined by TRLFS at 266 nm and 355 nm pulse laser excitations. Using fluorescence characteristics, a variety of different fuel sources could be distinguished. The studies have shown that under constant experimental conditions, the fluorescence lifetime at each emission wavelength is dependent on the interaction between fluorophores and non-fluorescent substances in diesel fuels. The time-resolved fluorescence spectra can show the main fluorescence characteristics of diesel fuels. Therefore, fluorescence allows you to distinguish the lifetime of diesel fuels.

The PCA method used as the pre-processing could provide a very intuitive analysis for different diesel fuels. Compared to U-PCA which requires to process the whole three-dimensional spectral information, the proposed method can significantly reduce the amount of data.

Compared to the traditional analytical methods such as GC-MS, HPLC, etc., the TRLFS method provides faster and more accurate distinction and does not require sample preparation. By considering these advantages, it can be used at the gas station or in the car, for example to prevent misfuelling and to provide in-situ information of the diesel fuels and biodiesel content for the engine control system of the vehicle.

In addition, by determination of fluorescence intensity at characteristic emission wavelengths, the content of diesel fuels and biodiesel in the blends can be quickly and easily quantified. This has a major significance for optimizing vehicle performance and reducing engine emissions. In contrast to the measurement at 266 nm laser excitation, the detectable fluorescence emission of biodiesel at 355 nm laser excitation was found. Also noted for the different biodiesel blends, the relationships between biodiesel content and the fluorescent intensity at a specific wavelength are unique and are caused by fluorescence of fluorophores and also by the fluorescence quenching-effect of fossil diesel and biodiesel. By comparison, with a calibration dataset of fluorescence at three characteristical emission wavelengths (422 nm, 438 nm and 525 nm), biodiesel in biodiesel blends in most instances (over 90 %) could not only be identified but also quantified.

To optimize the method the measuring range of the detector and the excitation wavelength of the laser source must be varied. On the global market other FAME, e.g. palm oil methyl ester (PME), coconut oil methyl ester (CME) and used cooking oil methyl ester (UCOME) are also relevant. Their impact on fluorescence must be investigated, too.

Because the huge variety of fossil diesels especially regarding aromatics the accuracy of biodiesel quantification in blends is the main challenge.

Acknowledgements

This work was financially supported by Fachagentur Nachwachsende Rohstoffe e.V. (FNR), "Fluoreszenzspektroskopische Charakterisierung und Identifizierung von Kraftstoffgemischen zur Entwicklung eines Kraftstoffsensors (TRLFS) – Project 22004710." We also thank the Thünen Institute of Agricultural Technology for support and the supply of biofuel blends.

Appendix A

Fuel data in accordance with CEC RF-06-03 of the fossil diesel fuels used (DF_{Ref})

Properties	Methods *DIN EN*	Units	Limit *Min.*	Limit *Max*	DF_{Ref}
cetane number	ISO 15195	-	52	54	53.4
cetane index	ISO 4264	-	46	-	
density (15 °C)	ISO 12185	kg/m³	833	837	834.3
polycyclic aromatic hydrocarbon	ISO 12916	% (m/m)	3	6	4.6
sulphur content	ISO 20884	mg/kg	-	10	3
flashpoint	ISO 2719	°C	> 55	-	92
carbon residue	ISO 10370	% (m/m)	-	0.2	< 0.01
ash content	ISO 6245	% (m/m)	-	0.01	< 0.001
water content	ISO 12937	mg/kg	-	200	23
total contamination	ISO 12662	mg/kg	-	20	
copper strip corrosion (3 h to 50 °C)	ISO 2160	degree of corrosion	1	1	1A
oxidation stability	ISO 12205	g/m³	-	25	< 1
HFRR (at 60 °C)	ISO 12156-1	µm	-	400	235
kin. viskosity (40 °C)	ISO 3104	mm²/s	2.3	3.3	3.126
CFPP	116	°C	-	-5	-17
distillation curve 95 % point	ISO 3405	°C	345	350	347.7
FAME content	ISO 14078	% (v/v)	-	-	best.
hydrogen	ASTM D 3343	%	-	-	13.74
carbon	ASTM D-3343	%	-	-	86.28
oxygen			-	-	-
caloric value	ASTM D 3338	MJ/kg	-	-	43.226
cloudpoint	EN 23015	°C	-	-	-15
neutralisation number	ASTM D 974	mg KOH/g	-	0.02	< 0.02
mono-aromatic	(IP 391)	% (m/m)	-	-	15.4
di--aromatic	(IP 391)	% (m/m)	-	-	4.6
tri+further	(IP 391)	% (m/m)	-	-	<0.1
total aromatics	(IP 391)	% (m/m)	-	-	20

Appendix B

Fuel data in accordance with DIN EN 14214 of the biodiesel fuels used (RME and SME)

Properties	Methods *DIN EN*	units	Limit *Min.*	Limit *Max*	RME	SME
ester content	14103	% (m/m)	96.5	-	98.2	98.4
density (15 °C)	ISO 12185	kg/m³	860	900	883.1	885.7
kin. viskosity (40 °C)	ISO 3104	mm2/s	3.5	5.0	4.458	4.123
flashpoint	ISO 3679	°C	101	-	182	168
CFPP	116	°C	-	0/-10/-20	-14	-6
sulphur content	ISO 20884	mg/kg	-	10.0	< 1	< 1
carbon residue	ISO 10370	% (m/m)	-	0.3	0.17	0.16
cetane number	15195		51		54	52.9
ash content	ISO 3987	% (m/m)	-	0.02	< 0.01	< 0.01
water content	ISO 12937	mg/kg	-	500	230	221
total contamination	12662	mg/kg	-	24	8	2
copper strip corrosion (3 h to 50 °C)	ISO 2160	degree of corrosion	1	1	1	1
oxidation stability	14112	h	6	-	8.4	6.5
acid number	14104	mg KOH/g	-	0.5	0.429	0.339
iodine number	14111	gr iodine/100gr	-	120	113	132
linolenic acid content	14103	% (m/m)	-	12	10	8.1
ME > = 4 double bonds	15779		-	1	0.06	0.09
methanol content	14110	% (m/m)	-	0.20	0.01	0.01
free glycerol	14105	% (m/m)	-	0.02	0.02	< 0.01
Monoglyzerides	14105	% (m/m)	-	0.80	0.8	0.7
diglycerides	14105	% (m/m)	-	0.20	0.2	0.11
triglycerides	14105	% (m/m)	-	0.20	0.2	0.01
total glycerine content	14105	% (m/m)	-	0.25	0.25	0.2
phosphorous content	14107	mg/kg	-	10	4	< 0.5
alkali content	14538	mg/kg	-	5	5	< 0.5
alkaline earth content	14538	mg/kg	-	5	5	< 0.5

References

Abdi H, Williams LJ (2010) Principal component analysis. Wiley Interdis Rev / Comput Statistics 2:433-459

Barbini R, Fantoni A, Palucci A, Ribezzo S, van der Steen HJL (1992) Spectral and time resolved measurements of pollutants on water surface by a XeC1 laser fluorosensor [online]. To be found at <http://www.earsel.org/Advances/1-2-1992/1-2_08_Barbini.pdf> [quoted 04.03.2015]

Bockey D (2013) Biodiesel 2012/2013 : report on the current situation and prospects ; abstract from the UFOP Annual Report [online]. To be found at <http://www.ufop.de/files/4413/8209/5819/WEB_UFOP_AuszugBiodiesel_13_EN.pdf> [quoted 04.03.2015]

Bünting UH(1999) Auswertungemethoden für die zeitaufgelöste Fluoreszenzspektroskopie. Göttingen : Univ, 153 p

Caires ARL, Lima VS, Oliveira SL (2012) Quantification of biodiesel content in diesel/ biodiesel blends by fluorescence spectroscopy : evaluation of the dependence on biodiesel feedstock. Renew Ener 46:137-140

Camagni P, Colombo A, Koechler C, Omenetto N, Qi P, Rossi G (1991) Fluorescence response of mineral oils: spectral yield vs absorption and decay time. Appl Optics 30(1):26-35

Chuck CJ, Bannister CD, Hawley JG, Davidson MG (2010) Spectroscopic sensor techniques applicable to real-time biodiesel determination. Fuel 89(2):457-461

Dumke I, Teschner M (1988) Application of fluorescence spectroscopy to geochemical correlation problems. Organic Geochem 13:1067-1072

Eftink MR (1991) Fluorescence quenching : theory and applications. In: Lakowicz JR (ed) Topics in fluorescence spectroscopy. New York : Plenum Pr, pp 53-126

Eftink MR, Ghiron CA (1981) Review of fluorescence studies with proteins. Anal Biochem 114(2):199-227

Fan Z, Krahl J (2013) Characterization and identification of diesel fuels, biodiesel and their blends by time-resolved laser-induced fluorescence spectroscopy, In: AMA Conferences 2013 proceedings : Nürnberg Exhibition Centre, Germany, 14.-16.52013 ; with SENSOR, OPTO, IRS2. Wunstorf : AMA Service, pp 432-436

Fan Z, Schröder O, Bär F, Eskiner M, Schaper K, Krahl J (2013) Fluoreszenzspektroskopische Charakterisierung und Identifizierung von Kraftstoffgemischen zur Entwicklung eines Kraftstoffsensors (TRLFS) : Förderkennzeichen: 22004710. Coburg : Coburg Univ Appl Sci Arts, 117 p

Foglia TA, Jones KC, Phillips JG (2005) Determination of biodiesel and triacylglycerols in diesel fuel by LC. Chromatographia 62(3/4): 115-119

Glover CJ, Bullin JA (1989) Identification of heavy residual oils by GC and GC-MS. J Environ Sci Health A 24(1):57-75

Grinvald A, Steinberg IZ (1974) On the analysis of fluorescence decay kinetics by the method of least-squares. Anal Biochem 59(2):583-598

Guimet F (2005) Olive oil characterization using excitation-emission fluorescence spectroscopy and three-way methods of analysis. Tarragona : Univ Rovira i Virgili

Hegazi E, Hamdan A (2002) Estimation of crude oil grade using time-resolved fluorescence spectra. Talanta 56:989-995

Hegazi E, Hamdan A, Mastromarino J (2005) Remote fingerprinting of crude oil using timeresolved fluorescence spectra. Arab J Sci Eng B 30(1):1-12

Hengstermann T, Reuter R (1980) Lidar fluorosensing of mineral oil spills on the sea surface. Appl Optics 29(22):3218-3327

Henrion R (1994) N-way principal component analysis theory, algorithms and applications. Chemometr Intell Lab Syst 25:1-23

Jacob I, Krahl J, Gnuschke H (2006) Einsatz der zeitaufgelösten Laserfluoreszenz-Spektroskopie bei der Analyse partikelgebundener PAK : Abschlussbericht. Coburg : Fachhochschule Coburg, 67 p

Jolliffe IT (2002) Principal component analysis. New York : Springer, 487 p

Khorasani GK (1987) Novel development in fluorescencemicroscopy of complex organic mixtures : application in petroleumgeochemistry. Org Geochem 11;157-168

Knothe G (2001) Historical perspectives on vegetable oil-based diesel fuels [online]. To be found at <https://www.oakland.edu/upload/docs/energy/inform_Nov_2001.pdf> [quoted 03.03.2015]

Kongbonga YGM, Ghalila H, Onana MB, Majdi Y, Lakhdar ZB, Mezlini H, Sevestre-Ghalila S (2011) Characterization of vegetable oils by fluorescence spectroscopy. Food Nutr Sci 2:692-699

Kulkarni BM, Pujar BG, Shanmukhappa S (2008) Investigation of acid oil as a source of biodiesel. Indian J Chem Technol 15:467-471

Kyriakidis NB, Skarkalis P (2000) Fluorescence spectra measurement of olive oil and other vegetable oils. J AOAC Int 83(6):1435-1239

Lakos Z, Szarka A, Koszorus L, Somogyi B (1995) Quenching-resolved emission anisotropy : a steady state fluorescence method to study protein dynamics. J Photochem Photobiol B 27:55-60

Lakowicz JR (2010) Principles of fluorescence spectroscopy. 3th Edition New York : Springer, 954 p

Lakowicz JR, Cryczynski I, Laczko G, Gloyna D (1991) Picosescond fluorescence lifetime standards for frequency- and time-domain fluorescence. J Fluoresc 1:87-93

Lampert RA, Chewter LA, Phillips D, O'Connor DV, Roberts AJ (1983) Standards for nanosecond fluorescence decay time measurements. Anal Chem 55:68-73

Lechner M, Bauer-Plank C, Lorbeer E (1997) Determination of acylglycerols in vegetable oil methyl esters by on-line normal phase LC–GC. J High Resolut Chromatogr 20:581-585

Ma XL, Sakanishi K, Isoda T, Nagao S, Mochida I (1996) Structural characteristics and removal of visible-fluorescence species in hydrodesulfurized diesel oil. Energy Fuels 10(1):91-96

Martens H, Naes T (1998) Multivariate calibration based on the linear mixture model. In: Martens H, Naes T (eds) Multivariate calibration. Chichester : Wiley, pp 166-213

Munack A, Krahl J (eds.) (2003) Erkennung des RME-Betriebes mittels eines Biodiesel-Kraftstoffsensors. Braunschweig : FAL, 76 p, Landbauforsch Völkenrode SH 257

Optimare (2005) OPTIMOS & OPTIMOS-Midi operation manual

Patsayeva S, Yuzhakov V, Varlamov V, Barbini R, Fantoni R, Frassanito C, Palucci A (2000) Laser spectroscopy of mineral oils on water surface. EARSeL eProceedings 1(1):106-115

Pearson K (1901) On lines and planes of closest fit to systems of points in space. Philosoph Magazine 2(6):559-5721)

Plank C, Lorbeer E (1995) Simultaneous determination of glycerol and mono-di-triglycerides I vegetable oil methyl esters by capillary LC-GC. J Chromatogr A 697:461-468

Quinn MF, Alotaibi AS, Sethi PS, Albahrani F, Alameddine O (1994) Measurement and analysis procedures for remote identification of oil spills using a laser fluorosensor. Int J Remote Sensing 15(13):2637-2658

Ralston CY, Wu X, Mullins OC (1996) Quantum yields of crude oils. Appl Spectrosc 50:1563-1568

Ryder AG, Glynn TJ, Feely M, Barwise AJ (2002) Characterization of crude oils using fluorescence lifetime data. Spect Act A 58:1025-1038

Sayago A, Morales MT, Aparicio R (2004) Detection of hazelnut oil in virgin olive oil by a spectrofluorimetric method. Eur Food Res Technol 218(5):480-483

Scherer MD, Oliveira SL, Lima SM, Andrade LH, Caires AR (2011) Determination of the biodiesel content in diesel/biodiesel blends : a method based on fluorescence spectroscopy. J Fluoresc21(3):1027–1031

Schmid U (2009) Entwicklung chemometrischer Methoden für die Klassifikation von Bakterien mittels Mikro-Raman-Spektroskopie. Braunschweig : Techn Univ, 205 p

Scott SM, James D, Ali Z, O'Hare WT, Rowell FJ (2003) Total luminescence spectroscopy with pattern recognition for classification of edible oils. Analyst 128(7):966-973

Sikorska E, Khmelinskii I, Sikorski M (2012) Analysis of olive oils by fluorescence spectroscopy : methods and applications. Intech Open Access Publ

Somoogyi B, Lakos Z (1993) Protein dynamics and fluorescence quenching. J Photochem Photobiol B 18:3-16

Steffens J, Landulfo E, Courrol LC, Guardani R (2011) Application of fluorescence to the study of crude petroleum. J Fluoresc 21:859-864

Terzic M, Marinkovic BP, Sevic D, Jureta J, Milosavljevic AR (2008) Development of time-resolved laser-induced fluorescence spectroscopic technique for the analysis of biomolecules. Facta universitatis / Physics Chemistry Technol 6(1):105-117

Vandeginste BGM, Massart DL, Buydens LMC, de Jong S, Lewi PJ, Smeyers-Verbeke J (1998) Handbook of chemometrics and qualimetrics : part B. Amsterdam : Elsevier

Westerhuis JA, Kourti T, MacGregor JF (1999) Comparing alternative approaches for multivariate statistical analysis of batch process data. J Chemom 13:397-413

Zawadzki A, Shrestha DS, He B (2007) Biodiesel blend level detection using ultraviolet absorption spectra. Trans Am Soc Agric Eng 50(4):1349-1353